Foodways in early farming societies: microwear and starch grain analysis on experimental and archaeological grinding tools from Central China

Li, W.

Appendix I Explanations of the variables used for describing microwear traces on grinding tools

1.1 Micro-striations

The term "striation", was first used by Semenov (1964) to describe traces found on archaeological artefacts and ethnographic objects. Striations refers to grooves and scratches of varying dimensions (Jensen 1988). Striations on ground stone tools are usually "caused by the movement of a harder surface across a softer one" (Adams et al. 2009:49). Linear traces such as micro-striations, gouges, and troughs are often encountered by microwear specialists on grinding tools associated with processing hard materials (e.g. metal and flint, Figure 1 and 2). Micro-striations can also form on grinding tools associated with cereal processing, especially near the margins of the tools due to direct contact between upper and lower grinding tools (Adams et al 2009; Li et al. 2019). Micro-striations can be described according to their length, width, and depth as long, short, narrow, wide, shallow, or deep (Table 1). The directionality of striations can be described as parallel, or multi-directional (Figure 3, Table 1). The directionality of parallel striations (e.g. parallel or perpendicular to the long axis of the tool, Table 1) can be used to indicate the grinding motion (e.g. reciprocal or rotary motion).

1.2 Micro-polish

Micro-polish was first observed on flint tools and studied by a number of scholars (Semenov 1964; Newcomer and Keeley 1977; Keeley 1980; Vaughan 1985; Van Gijn 1990). Following Plisson (1985), Adams et al. (2009:54) defined micro-polish as "a modification of the microtopography of a tool's surface taking the form of a smooth and even sheen that reflects light differently than an unmodified rock". The framework established for analysing flint tools can be adapted to study archaeological grinding tools, as proposed by Dubreuil and Savage (2014). In the present dissertation, different types of micro-polish are documented in terms of their topography, texture, general appearance, location, polish development, degree of linkage, brightness, and directionality.

Terms such as flat, sinuous, domed, and irregular are used to describe the topography of observed micro-polish (Table 1, Figure 4). For instance, micro-polish associated with processing stone and metal materials is flat (Figure 1), while micro-polish resulting from processing, wood, bone, and hide has a sinuous to domed topography (Figure 5 and 6). Contact with clay results in the development of a dull micro-polish of rough texture and irregular morphology (Tsoraki et al. in preparation) (Figure 7).

The texture and general appearances of various types of polish can be described as smooth, rough, pitted, spider-web like (Van Gijn and Verbaas 2007), or greasy. For example, the texture of micro-polish developed from contact with bone and wood is smooth while hide micro-polish is smooth on the higher micro-topography and appears rough in the lower micro-topography (Figure 5, 6, and 8). These three different types of micro-polish can be further distinguished according to other features (e.g. location, brightness, and presence of linear features etc., see below)(Adams et al. 2009; Hayes et al. 2018; Tsoraki et al. in preparation).

Polish can develop in different locations on stone tool surfaces (e.g. higher micro-topography, intermediate area, lower micro-topography). In the case of bone and wood processing, polish appears mainly on the higher micro-topography due to the hardness and inflexibility of the processed materials (Figure 5 and 8). Polish resulting from contact with hide, however, occurs on the higher and lower micro-topography (Figure 6).

Brightness of polish can be described as dull, medium reflective, or highly reflective. For instance, polish resulting from processing clay is typically dull (Figure 7), while polish resulting from processing metal has a highly reflective appearance (Figure 1). Comparing to polish resulting from wood processing (Figure 8), polish associated with processing dry bone is more reflective, especially for the well-developed polish (Figure 5). Bone micro-polish can also be associated with troughs (linear features) (Figure 5).

Polish can develop on tool surfaces in different ways, i.e., on individual grains (localised distribution), in patches (of linear or random disposition), band/ streak, continuous across a large surface (Tsoraki et al. in preparation) (Table 1). Processing cereals with grinding tools usually develops polish in individual grains and gradually forms patches (Figure 9). Differently, processing clay forms polish that is continuous across a large surface (Figure 7). For polish that has formed in patches, a degree of linkage can be used to describe whether these patches are separated or well-linked. The degree of linkage can be judged by looking at the distributions of different patches (Figure 10).

Similar to directionality of striations, directionality of polish can also be used to indicate different types of grinding motions. For example, a grinding slab and roller used with a back and forth motion, the direction of the resulting polish is parallel to the long axis of a grinding slab and perpendicular to the long axis of the corresponding grinding roller.

In addition to striations and micro-polish, other features such as micro-fractures, grain (edge) rounding, and levelling of grains also allow microwear specialists to interpret the contact material (Dubreuil et al. 2015; Tsoraki et al. in preparation). Furthermore, documentation of residues while doing microwear analysis enriches

our understanding of the potential possessed material as well as post-depositional processes of an artefact (Dubreuil et al. 2015).

For microwear analysis, as has been discussed by Semenov and many others (e.g. Semenov 1964; Keeley 1980; Levi Sala 1986; Jensen 1988), the cleaning procedures are essential before the observation of experimental implements. In the current dissertation, as some of the experimental grinding tools were also subjected to starch grain analysis, sampling for starch was conducted immediately after the completion of the grinding experiments (see Chapter 1, 3, and 5) and prior to cleaning. Following residue sampling, the experimental tools were cleaned in an ultrasonic bath. These tools were then washed with soap under running tap water in the Laboratory for Material Culture Studies at the Faculty of Archaeology, Leiden. The observations of the microwear traces were carried out after the experimental tools were completely dry.

Table 1: Wear features recorded

Variables		Description
Micro-striations	Directionality	parallel or vertical to the long axis of the tool
	Morphology	Wide, narrow, deep, shallow, long, short
Polish	Morphology	flat, sinuous, domed, irregular
	Texture and general appearance	smooth, pitted, rough, granular, spider-web like, greasy
	Location	higher micro-topography, intermediate area, lower micro-topography
	Brightness	dull, medium reflective, highly reflective
	Polish development	localised (limited distribution either on individual grains or on a small number of coalescing grains/grain aggregates), in patches (of linear or random disposition), band/ streak, continuous across a large surface
	Degree of linkage	well-linked patches or not
	Directionality	parallel to long axis, diagonal to long axis, or perpendicular to long axis

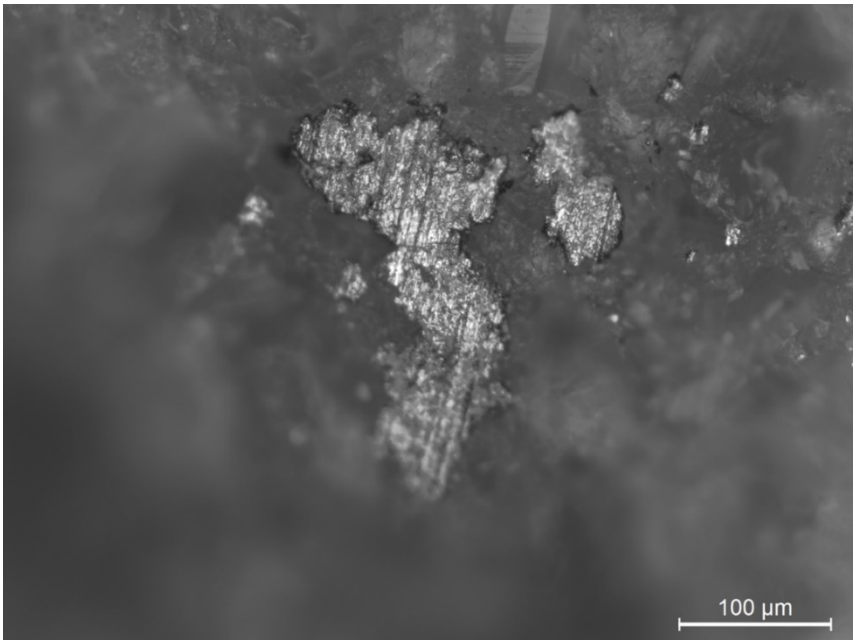

Figure 1 Microwear traces associated with the contact of bronze. The sandstone tool was used for polishing a bronze knife for 240 min (Experiment No. 1439, Laboratory for Material Culture Studies at Leiden University, © Weiya Li).

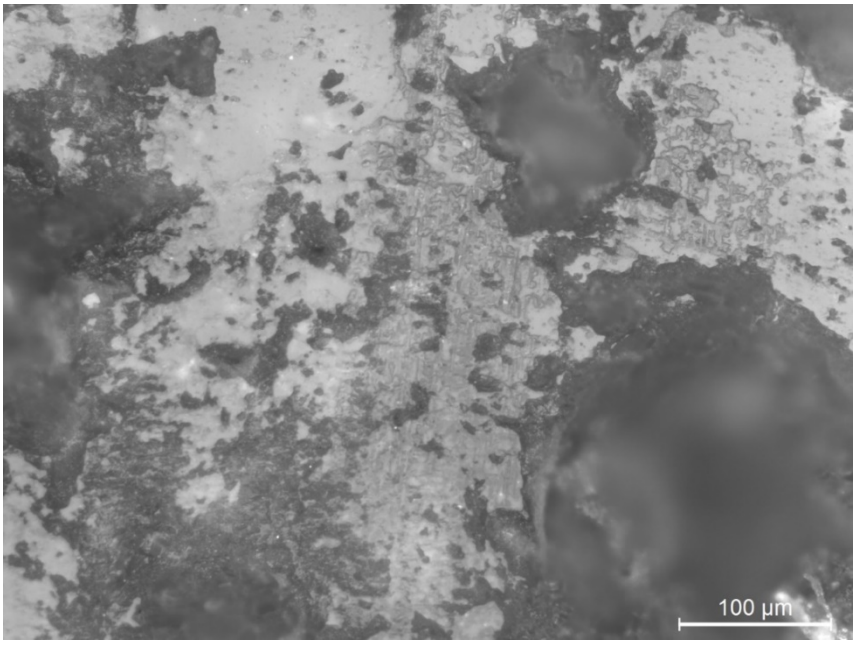

Figure 2 Microwear traces associated with the contact of flint. The sandstone tool was used for grinding flint for 180 min with water. (Experiment No. 1322, Laboratory for Material Culture Studies at Leiden University, © Weiya Li).

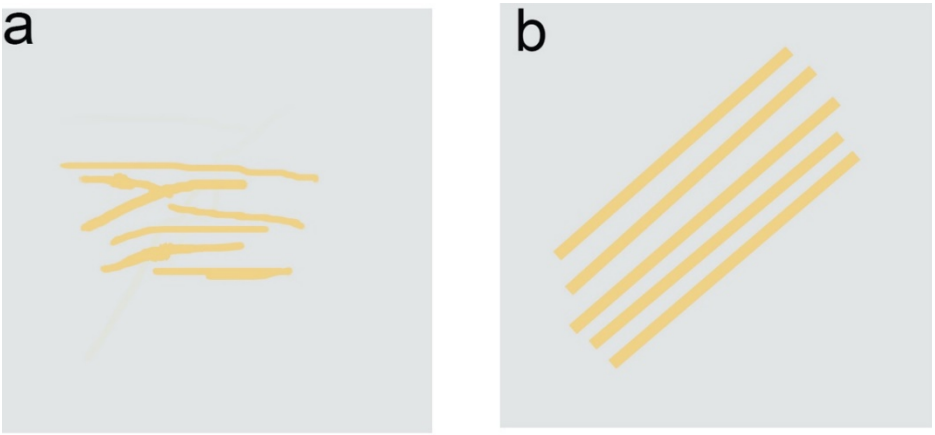

Figure 3 Illustrations of irregular striations (a) and paralleled striations (b) (After Wang, 2019)

Figure 4: Illustrations of micro-polish with (a) flat, (b) domed and sinuous, and (c) irregular topography (After Wang, 2019)

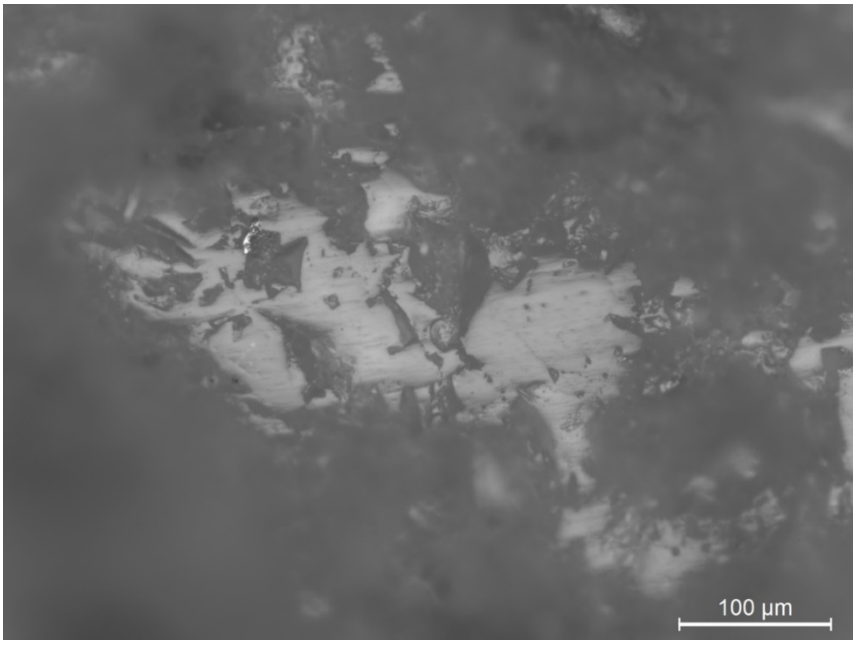

Figure 5 Microwear traces associated with the contact with dry bone. The sandstone tool was used for grinding dry bone for 180 min. (Experiment No. 3032, Laboratory for Material Culture Studies at Leiden University, © Weiya Li).

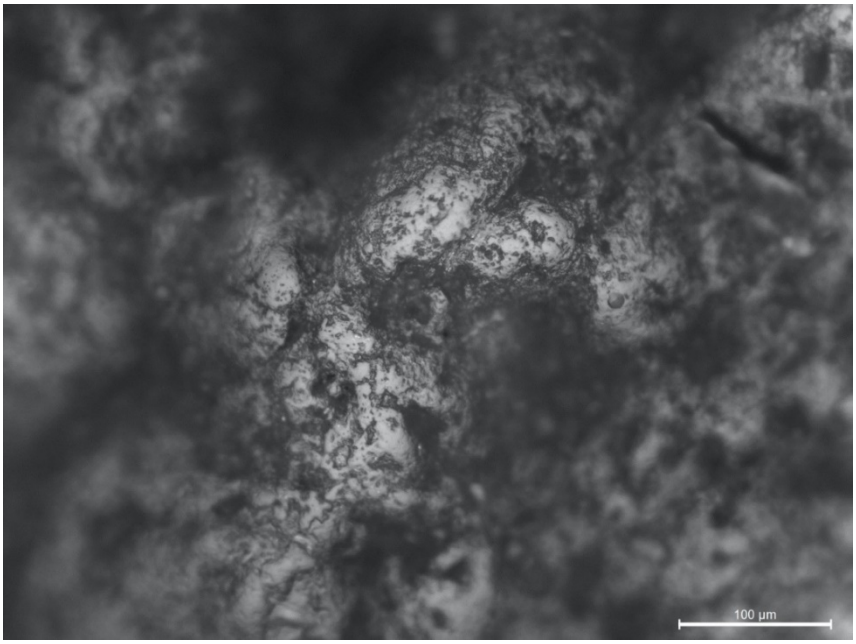

Figure 6 Microwear traces associated with hide processing. The sandstone tool was used for smoothing hide for 180 min. (Experiment No. 2586 Laboratory for Material Culture Studies at Leiden University, © Weiya Li).

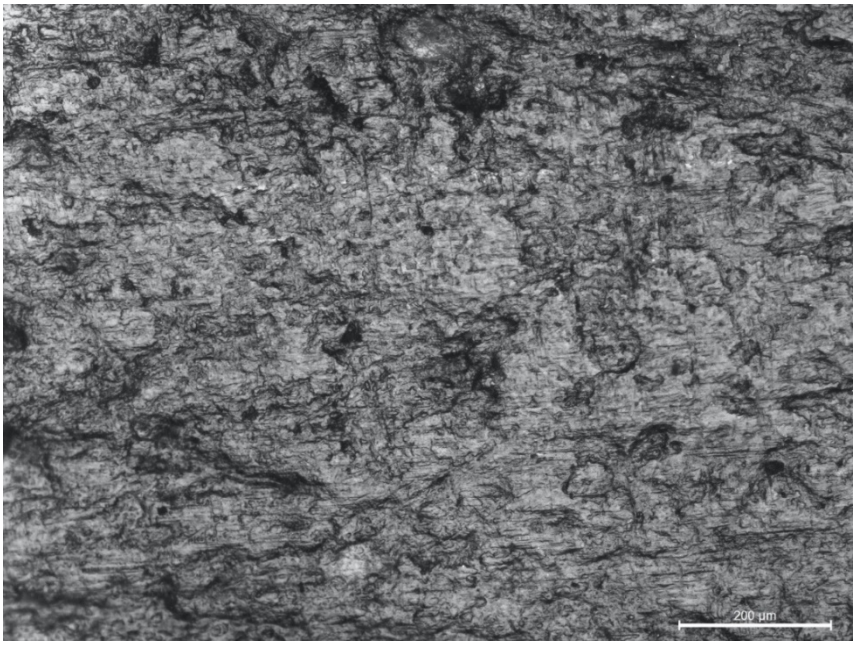

Figure 7 Microwear traces associated with processing clay. This sandstone tool was used for polishing clay for 325 min. (Experiment No. 983, Laboratory for Material Culture Studies at Leiden University, © Weiya Li).

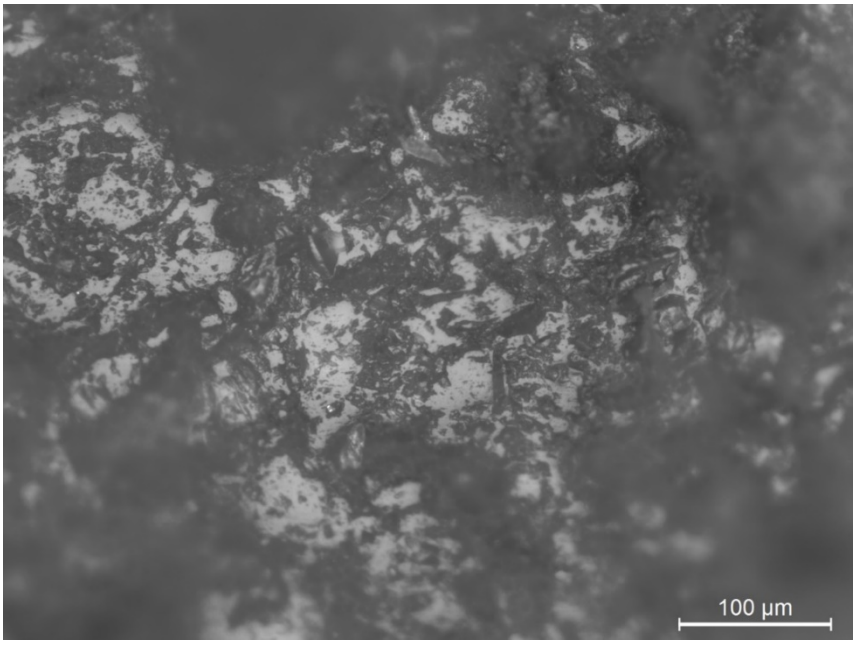

Figure 8 Microwear traces associated with wood processing, 3200 strokes (time unknown) in experimental machine load used 1.25 kg, sandstone tool (Experiment No. 1368, Laboratory for Material Culture Studies at Leiden University, © Weiya Li).

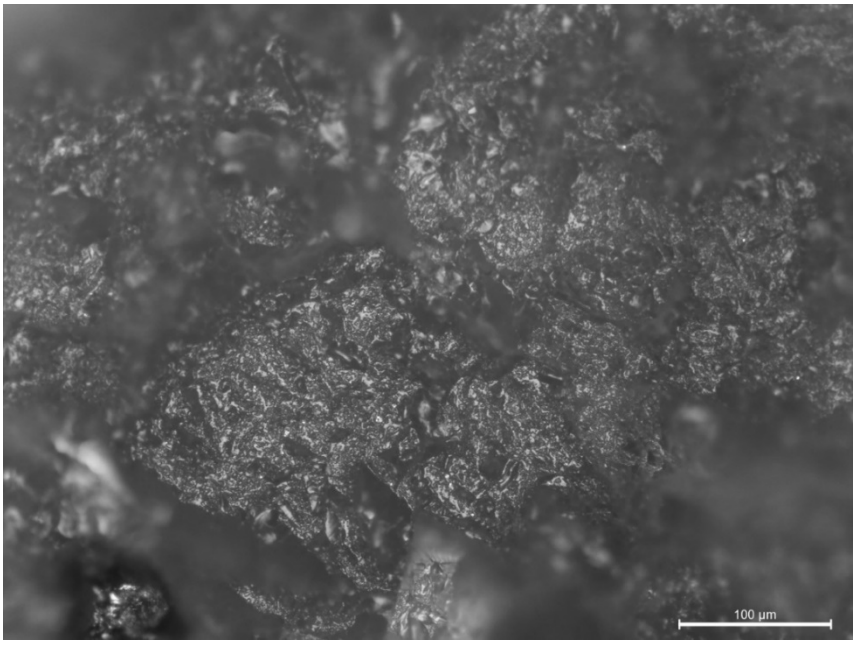

Figure 9 Microwear traces associated with processing foxtail millet for 180 min, sandstone tool (Experiment No. 2468, Laboratory for Material Culture Studies at Leiden University, © Weiya Li).

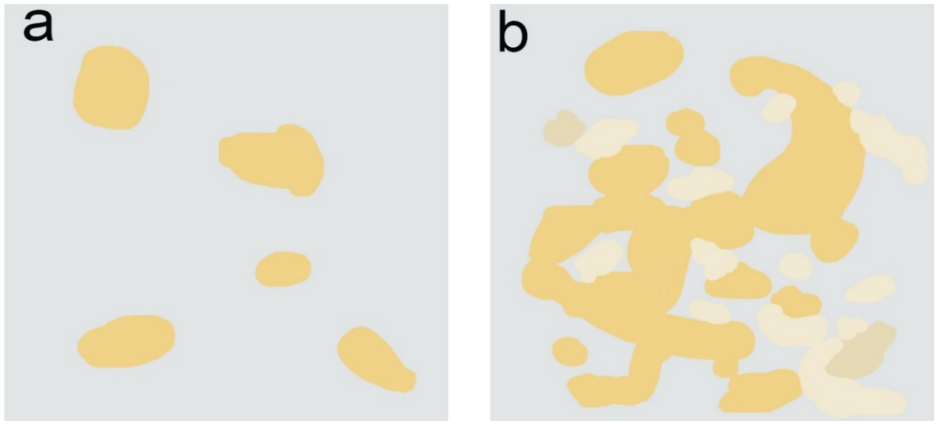

Figure 10 Illustration of polish patches that are separated (a) and polish patches that are well linked (b) (after Wang, 2019).

References

Adams, J., Delgado-Raack, S., Dubreuil, L., Hamon, C., Plisson, H., and Risch, R., 2009, Functional analysis of macro-lithic artefacts: a focus on working surfaces, In Non-flint Raw Material Use in Prehistory: Old Prejudices and New Directions (ed. L. E. and L. J. C. F. Sternke), 43–66, Archaeopress, BAR International Series 1939, Oxford.

Dubreuil, L., Savage, D., Delgado-Raack, S., Plisson, H., Stephenson, B., and de la Torre, I., 2015, Current Analytical Frameworks for Studies of Use–Wear on Ground Stone Tools, In Use-Wear and Residue Analysis in Archaeology, 105–58, Springer.

Van Gijn, A. L., 1990, The wear and tear of flint: principles of functional analysis applied to Dutch Neolithic assemblages, Analecta Praehistorica Leidensia 22.

Van Gijn, A., and Verbaas, A., 2007, Querns and other hard stone tools from Geleen Janskamperveld, In analecta Praehistorica leidensia, Vol. 39, 191–204, Faculty of Archaeology, Leiden University.

Hayes, E., Pardoe, C., and Fullagar, R., 2018, Sandstone grinding/pounding tools: Use-trace reference libraries and Australian archaeological applications, Journal of Archaeological Science: Reports, 20, 97–114.

Jensen, H. J., 1988, Functional analysis of prehistoric flint tools by high-power microscopy: A review of West European research, Journal of World Prehistory, 2(1), 53–88.

Keeley, L. H., 1980, Experimental determination of stone tool uses: a microwear analysis, University of Chicago press, Chicago.

Levi Sala, I., 1986, Use wear and post-depositional surface modification: A word of caution, Journal of Archaeological Science, 13(3), 229–44.

Li, W., Tsoraki, C., Lan, W., Yang, Y., Zhang, J., and van Gijn, A., 2019, New insights into the grinding tools used by the earliest farmers in the central plain of China, Quaternary International, 529, 10–7.

Newcomer, M., and Keeley, L. H., 1977, Microwear Analysis of Experimental Flint Tools: a Test Case, Journal of Archaeological Science, 4(4), 29–62.

Plisson, H., 1985, Etude fonctionnelle d'outillages lithiques préhistoriques par l'analyse des micro-usures: recherche méthodologique et archéologique, , Doctoral thesis at Université de Paris I.

Semenov, S. A., 1964, Prehistoric Technology, Adams and Dar, London.

Tsoraki, C., Verbass, A., and Van Gijn, A., The application of the high-power approach to the study of ground stone technology: towards a methodological framework, in preparation.

Vaughan, P. C., 1985, Use-wear analysis of flaked stone tools, University of Arizona Press, Arizona.

Wang, J., 2019, The Origin of Rice Agriculture in the Lower Yangtze Valley, China, , Doctoral thesis at Stanford University.

Appendix II Supporting data for Fig. 4.3b in Chapter 4

Table S4.1: Number of different types of starch grains after dry-grinding

Starch type / Plant species	Type I	Type II	Type III	Total
rice (n=6)	0	0	6	6
foxtail millet (n=60)	26	21	13	60
Job's tears (n=69)	47	6	16	69
barley (n=53)	19	11	23	53

Note: The images below (from Fig. S4.5 to Fig. S4.23) are the supporting data for table S4.1 and Figure 4.3b, the blue numbers in the images are used to count the total single starch grains, the yellow numbers are used to count Type I starch grains, and the red numbers are used to count Type II starch grains, the rest are Type III starch grains.

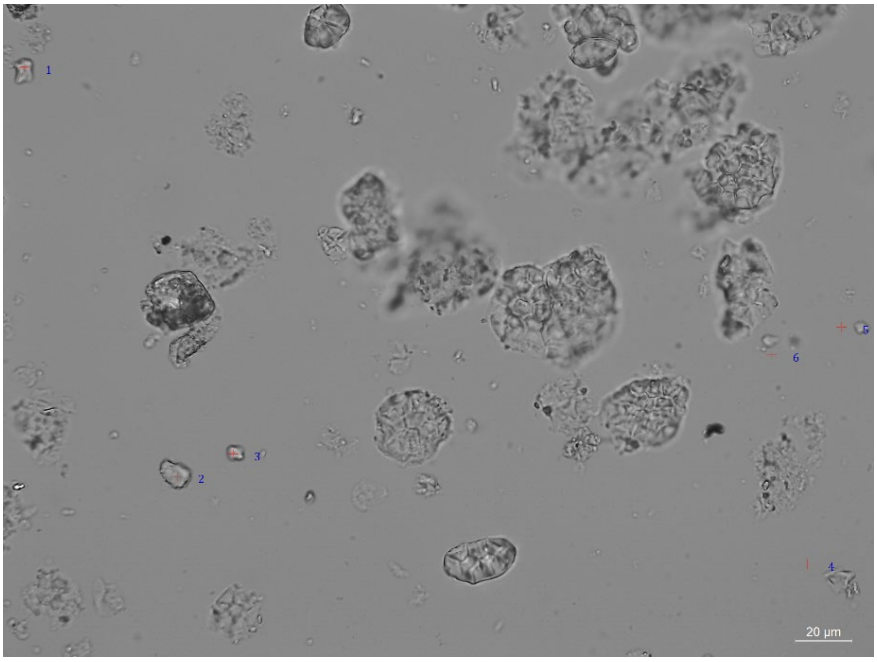

Figure S4.5. Starch grains from rice after dry-grinding under the bright field, Total number of single starch grains (n=6).

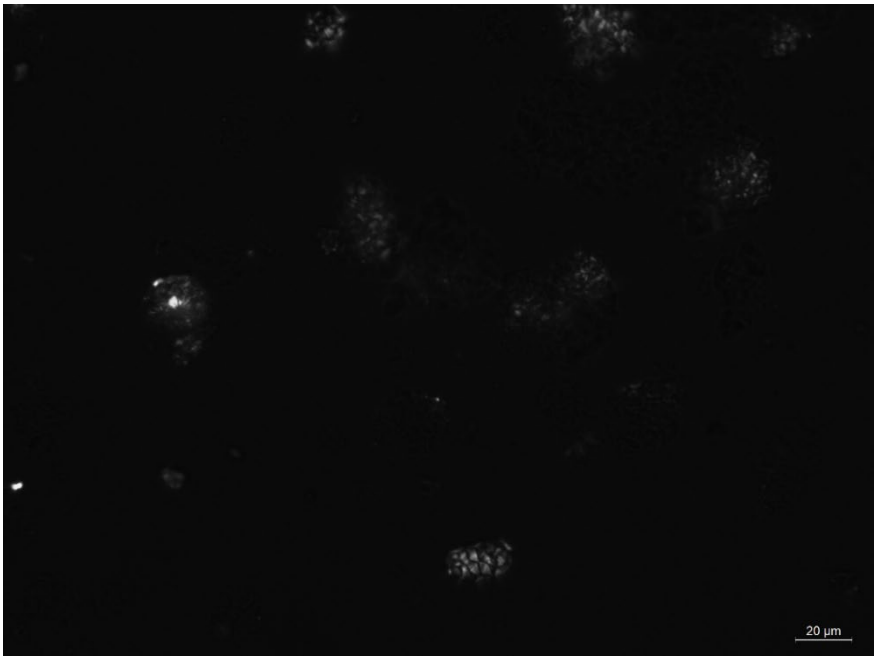

Figure S4.6. Starch grains from rice after dry-grinding under polarized light, note that all the single starch grains lost their extinction crosses. Type I starch grains (n=0); Type II single starch grains (n=0); Type III starch grains (n=6).

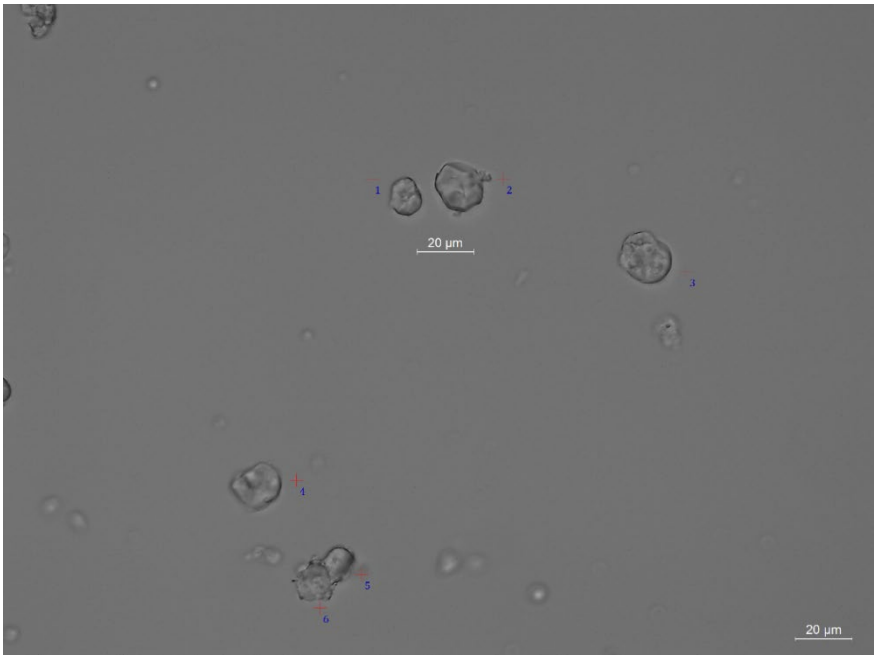

Figure S4.7. Starch grains from foxtail millet after dry-grinding under the bright field, Total number of single starch grains (n=6).

Figure S4.8. Starch grains from foxtail millet after dry-grinding polarized light, Type I starch grains (n=0); Type II single starch grains (n=4); Type III starch grains (n=2).

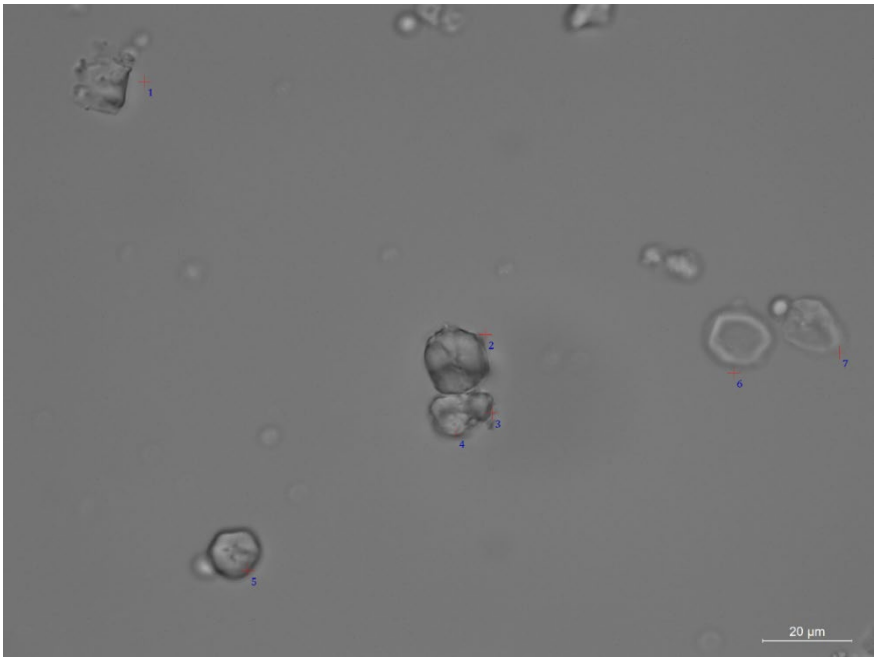

Figure S4.9 Starch grains from foxtail millet after dry-grinding under the bright field, the total number of single starch grains (n=7).

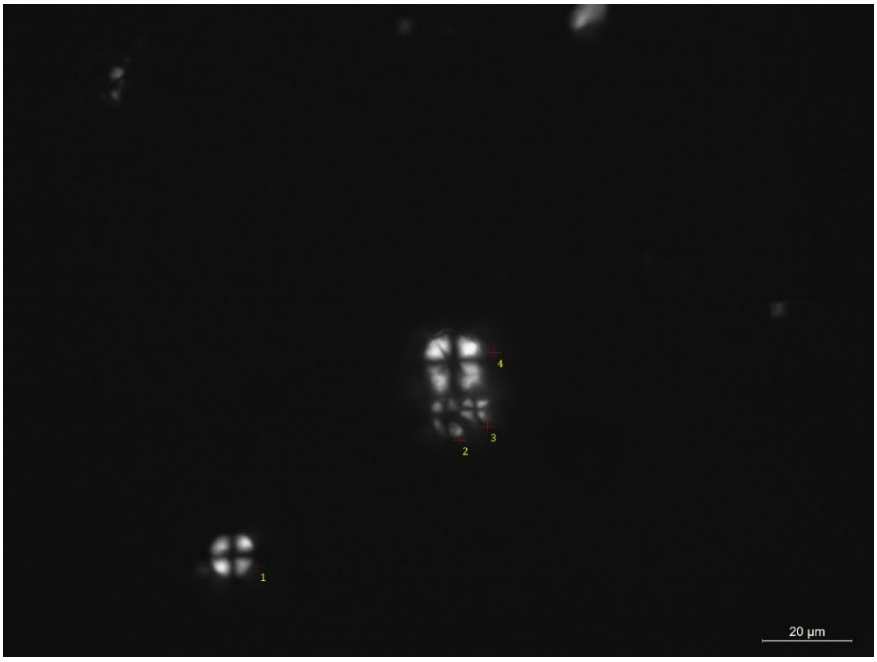

Figure S4.10 Starch grains from foxtail millet after dry-grinding polarized light, Type I single starch grains (n=4); Type II single starch grains (n=0); Type III starch grains (n=3).

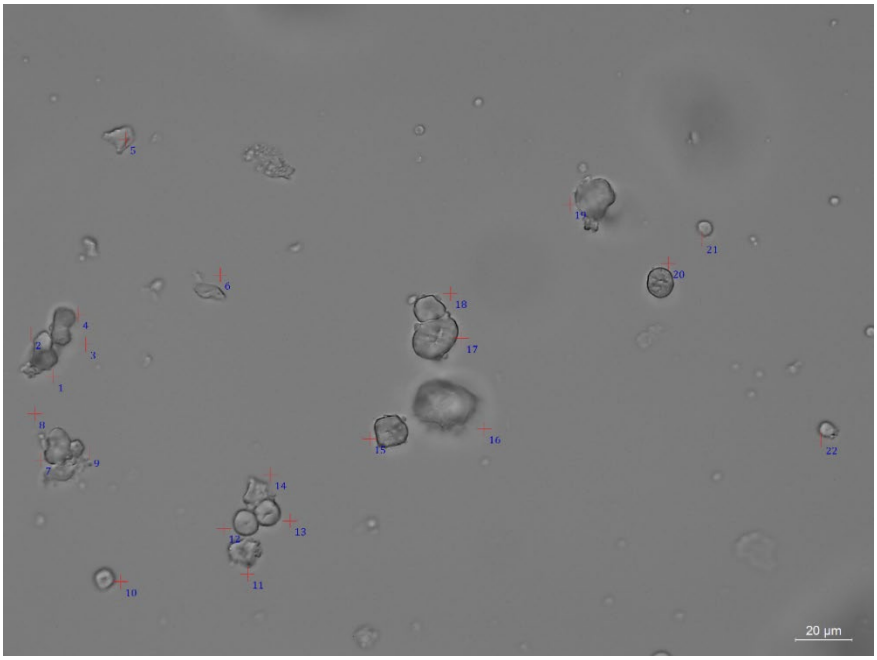

Figure S4.11 Starch grains from foxtail millet after dry-grinding under the bright field, the total number of single starch grains (n=21).

Figure S4.12 Starch grains from foxtail millet after dry-grinding polarized light, Type I single starch grains (n=10), Type II single starch grains (n=4); Type III starch grains (n=7).

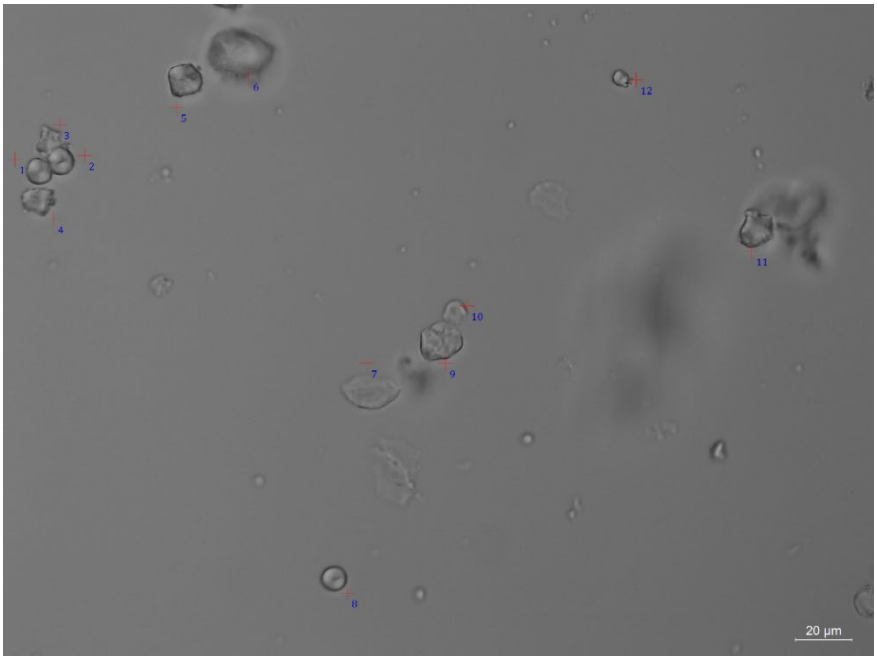

Figure S4.13 Starch grains from foxtail millet after dry-grinding under the bright field, the total number of single starch grains (n=12).

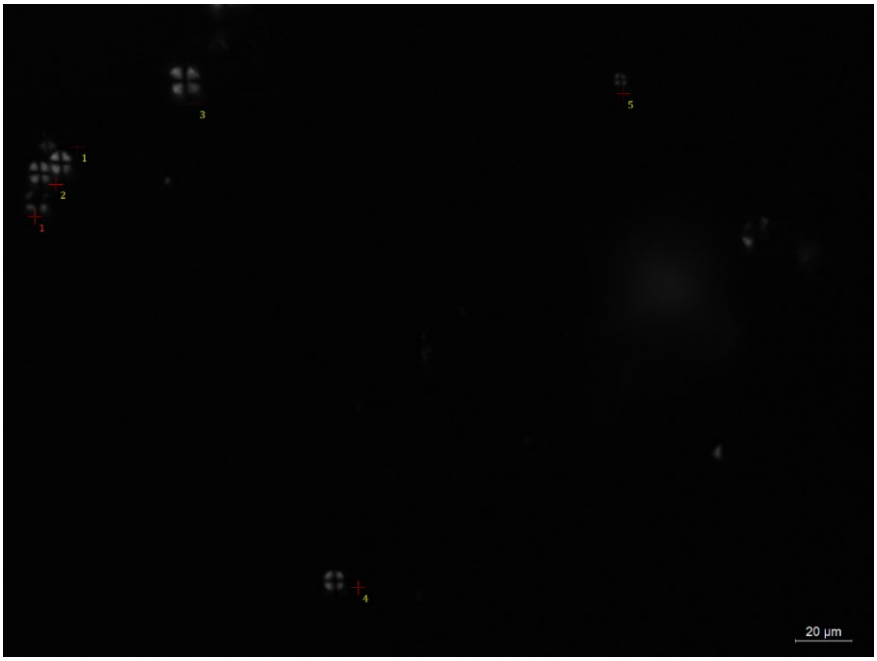

Figure S4.14 Starch grains from foxtail millet after dry-grinding polarized light, Type I single starch grains (n=5), Type II single starch grains (n=1); Type III starch grains (n=6).

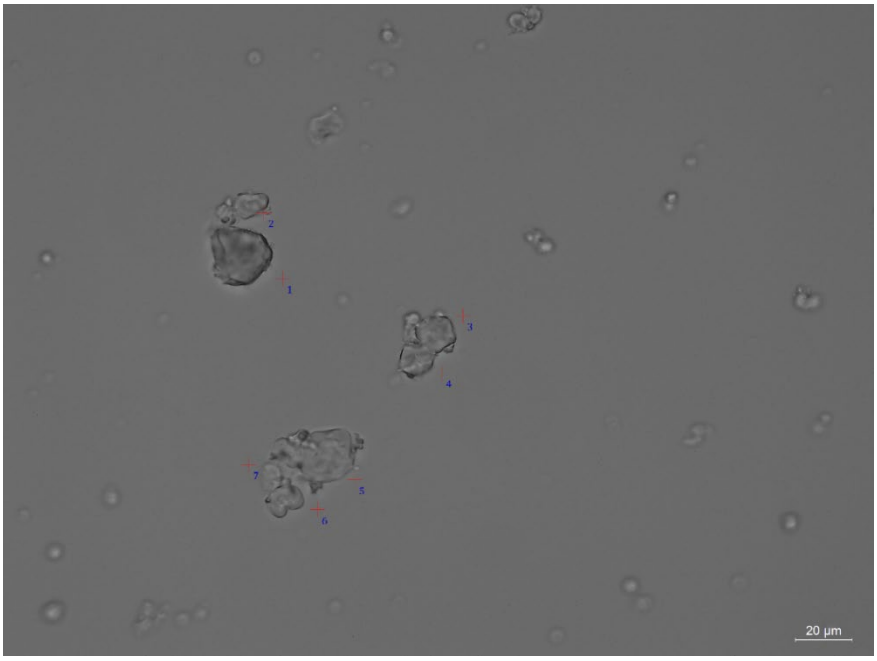

Figure S4.15 Starch grains from foxtail millet after dry-grinding under the bright field, the total number of single starch grains (n=7).

Figure S4.16 Starch grains from foxtail millet after dry-grinding polarized light, Type I starch grains (n=0); Type II single starch grains (n=2); Type III starch grains (n=5).

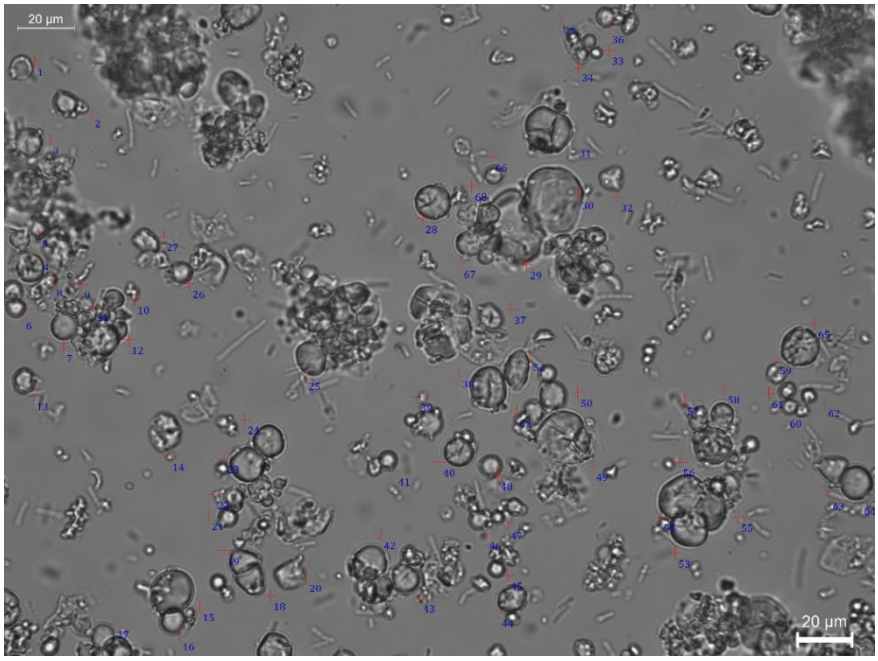

Figure S4.17 Starch grains from Job's tears after dry-grinding under the bright field, the total number of single starch grains (n=69).

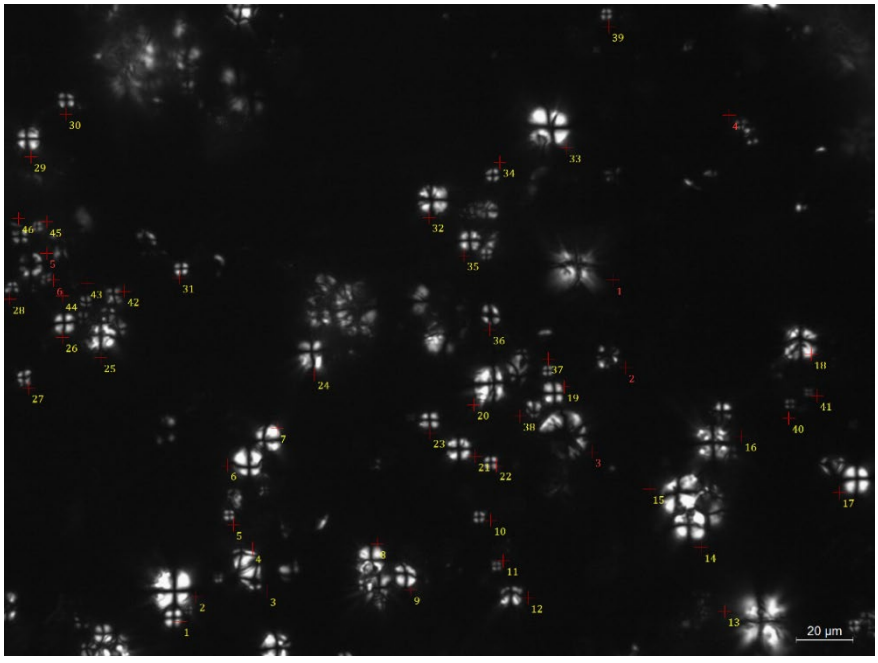

Figure S4.18 Starch grains from Job's tears after dry-grinding under the bright field, Type I single starch grains (n=47), Type II single starch grains (n=6); Type III starch grains (n=16).

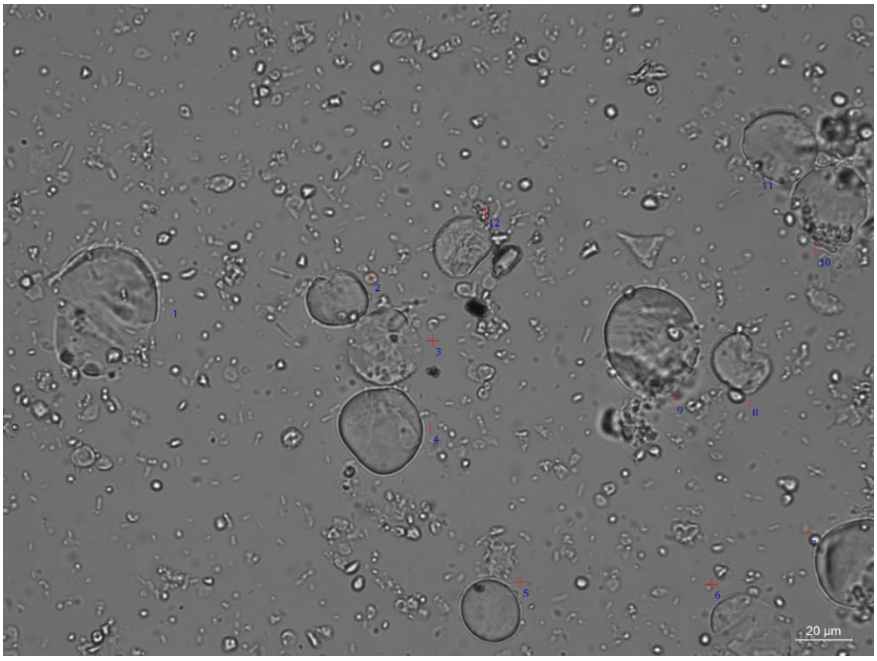

Figure S4.19 Starch grains from barley after dry-grinding under the bright field, the total number of single starch grains (n=12).

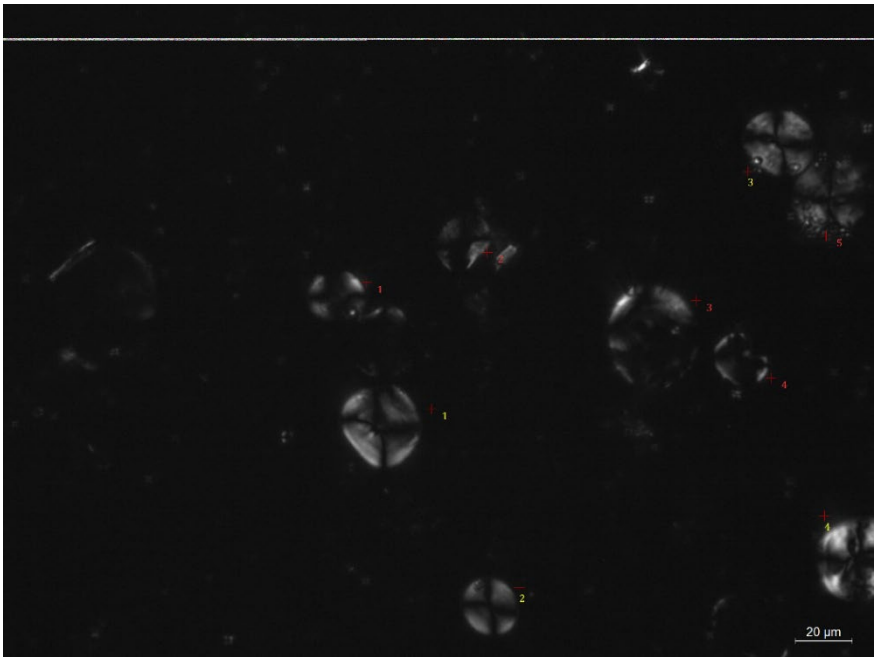

Figure S4.20 Starch grains from barley after dry-grinding under the bright field, Type I single starch grains (n=4), Type II single starch grains (n=5); Type III starch grains (n=3).

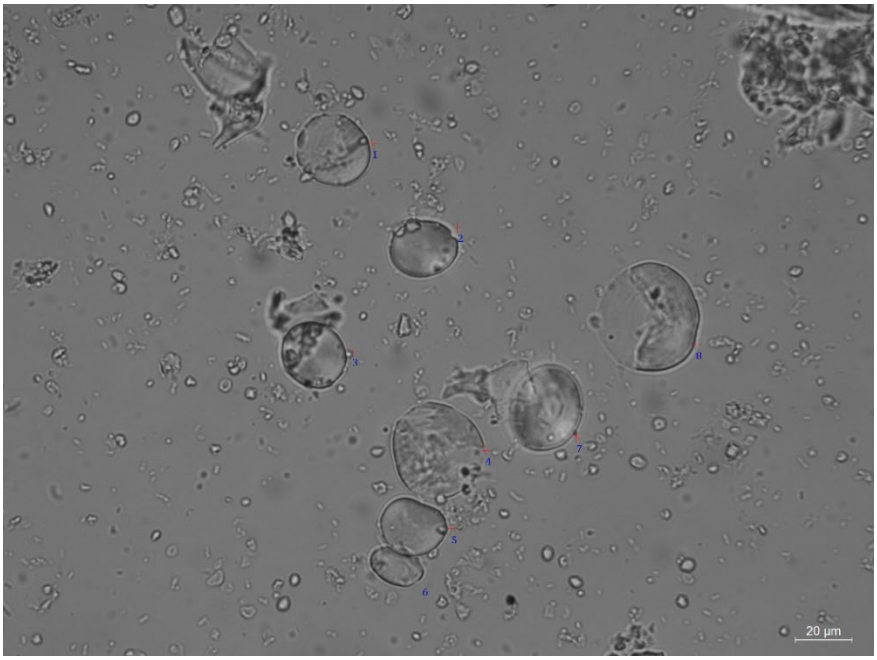

Figure S4.20 Starch grains from barley after dry-grinding under the bright field, the total number of single starch grains (n=8).

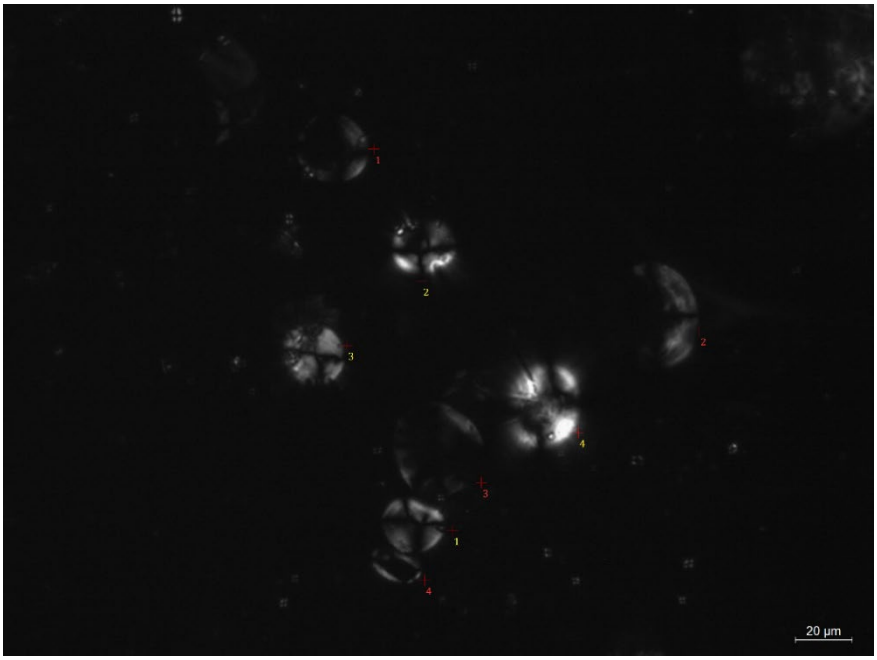

Figure S4.21 Starch grains from barley after dry-grinding under the bright field, Type I single starch grains (n=4), Type II single starch grains (n=4); Type III starch grains (n=0).

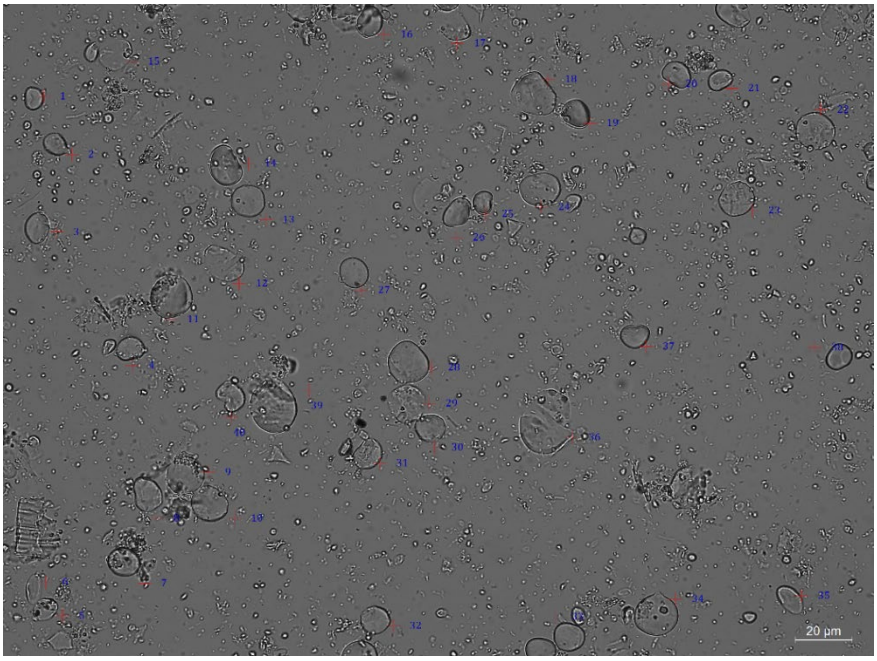

Figure S4.22 Starch grains from barley after dry-grinding under the bright field, the total number of single starch grains (n=40).

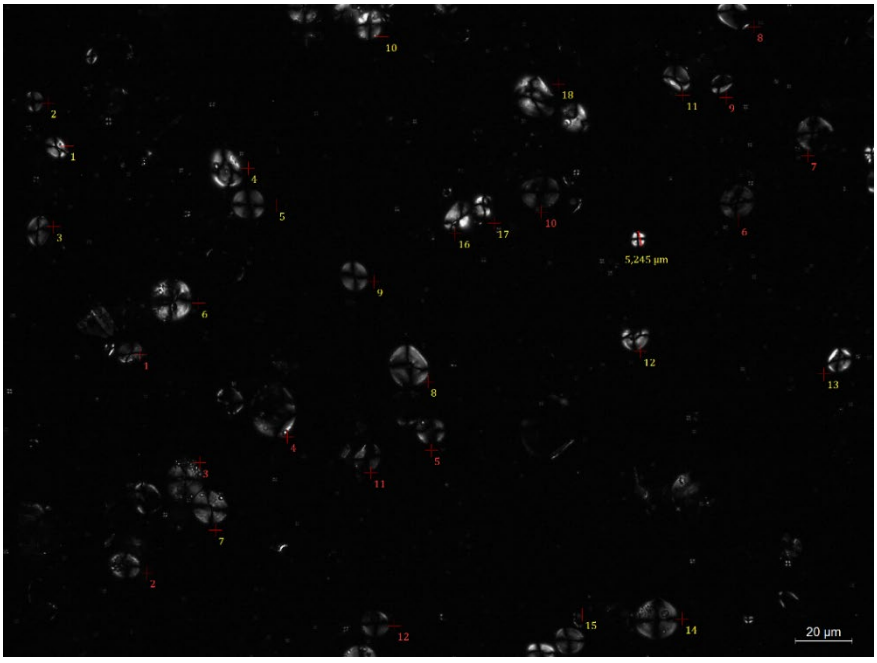

Figure S4.23 Starch grains from barley after dry-grinding under the bright field, Type I single starch grains (n=18), Type II single starch grains (n=12); Type III starch grains (n=10).